

SURVEY OF SUPERRESOLUTION USING PHASED BASED IMAGE MATCHING

¹BUDI SETIYONO, ²MOCHAMAD HARIADI, ²MAURIDHI HERY PURNOMO

¹Department of Mathematics Sepuluh Nopember Institute of Technology, Surabaya – Indonesia

²Department of Electrical Engineering Sepuluh Nopember Institute of Technology, Surabaya – Indonesia

E-mail: ¹masbudisetiyono@gmail.com, ²mochar@gmail.com, ²hery@ee.its.ac.id

ABSTRACT

Superresolution (SR) is a method of enhancing image resolution by combining information from multiple images. Two main processes in superresolution are registration and image reconstruction. Both of these processes greatly affect the quality image of the superresolution. Accurate registration is required to obtain high-resolution image quality. This research propose a collaboration between Phase-Based Image Matching (PBIM) registration, and reconstruction using Structure - Adaptive Normalized convolution algorithm (SANC) and Projection Onto Convex sets algorithm (POCs). PBIM was used to estimate translational registration stage. We used the function fitting around the peak point, to obtain sub pixel accurate shift. The results of this registration were used for reconstruction. Three registration method and two reconstruction algorithms have been tested to obtain the most appropriate collaboration by measuring the value of Peak Signal to Noise Ratio (PSNR). The result showed that the collaboration of PBIM and both reconstruction algorithm, SR with PBIM and POCs have PSNR average of 32.12205, while PSNR average of SR with SANC algorithm was 32.07325. For every collaborative algorithms that have been tested, registration PBIM with function fitting, has an higher average PSNR value than the Keren and Marcel registration.

Keywords: *Phased Based Image Matching, Reconstruction, Registration, Superresolution, SANC, POCs*

1. INTRODUCTION

Data or information is not only expressed in the form of text, but also may include multimedia as images, audio, and video. Image as one of the multimedia component holds very important role as a form of visual information. The higher resolution image provide more detailed information. Image with high resolution can be obtained by improving the quality of the CCD, but it is costly. Another approach is the superresolution. It is done by processing the signal, that require lower cost.

Superresolution (SR) is a method to improve the resolution of Low Resolution images (LR) into High Resolution image (HR). Based on the number of reference images are used, superresolution can be grouped into two categories. They are superresolution using an image, and superresolution using multiple images in the same scene as reference [1].

Some researches showed that the good reconstructions were strongly influenced by the registration process [1][2][3]. Phase Based Image Matching (PBIM) was used to estimate the translational registration stage, because of its high accuracy up to 0.01 pixel. Only translation with sub

pixel accuracy that contributed in the reconstruction process[4][5][6]. The research also showed that PBIM was better in performance, efficiency and complexity compared to the block-matching method.

Other researchers compared two registration techniques, algorithms based on nonlinear optimization and Discrete Fourier transform (DFTs). The results showed that after being compared with usual FFT approach, these algorithms have shorter computational time and also required less memory[7][8]

Several popular and powerful reconstruction algorithms that have been developed are the Structure-Adaptive Normalized convolution SANC[9][10]. The Structure-Adaptive Normalized convolution (SANC) algorithm is the image interpolation algorithms that work on the scope of Normalized convolution. This algorithm defines the applicable function based on the distance to the neighboring pixel point. Other reconstruction algorithm is the Projection Onto Convex Sets (POCs). The algorithm is effective for the reconstruction of image containing motion blur and has noise [11][12]. Several studies related to the superresolution have been conducted by researchers.[13][14][15][16][17].

In this research authors conducted a collaborative study between the registration and reconstruction process. The registration process used PBIM, while the reconstruction used two algorithm, such as SANC and POCs to find the best performance in producing high-resolution image. We fitted the data points around the peak point, to obtain more accurate shifting of the sub pixel. Block diagram in Figure 1 is the stages that performed in this research. In this study, superresolution began with taking objects using video. They were extracted to obtain a series of images in the same scene.. Then pixels translation was estimated using Phased Based Image Matching and fitted for the sub-pixel level shifting. In determining the effect of registration and reconstruction of objects which have different characteristics, we used some images that contain lots of texture and some other with less texture for experiment.

The authors also compared the accuracy of the PBIM registration with fitting and Keren and Marcel registration. The registration results were used for reconstruction using SANC and POCs algorithm This paper is organised as follows. Section 2 presents the problems related to superresolution and techniques registration using PBIM, and the fitting function to estimate the level of sub-pixel shifting. Section 3 presents a reconstruction algorithm using the SANC and POCs algorithm. Furthermore, section 4 describes the result and the discussion of collaboration between the registration and reconstruction. Finally, section 5 is a conclusion.

2. SUPERRESOLUTION

Superresolution has two main stages, which are the registration and reconstruction. The registration is done by estimating the pixels translation, which is useful for reconstruction. If the translation pixels is in integer, then each image will contain the same information. This cannot be used in superresolution. But if the translation level are in real pixels (sub pixels), it will obtain additional information that will be useful at the time of reconstruction. Figure 2 shows the step of the superresolution.

In this research, authors conducted collaboration between registration with PBIM and two reconstruction algorithms, Structure-Adaptive Normalized Convolution (SANC) and the Projection onto Convex Sets (POCs) algorithm.

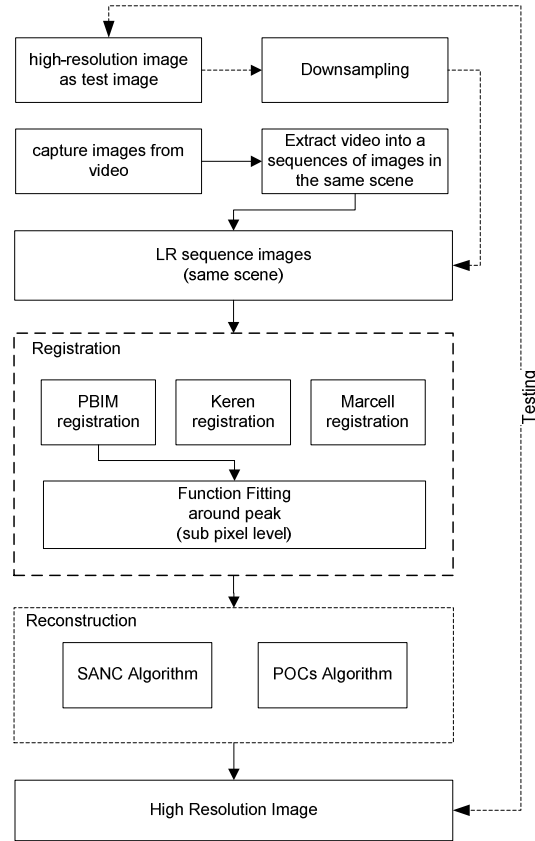


Figure 1. Block Diagram of Research

2.1. Phased Based Image Matching

Suppose there are two images $f(n_1, n_2)$ and $g(n_1, n_2)$ with dimensions $N_1 \times N_2$.

Assumed index n_1 ranged from $-M_1, \dots, M_1$ and n_2 ranged from $-M_2, \dots, M_2$. To simplify these indexes we used the equations $N_1 = 2M_1 + 1$ and $N_2 = 2M_2 + 1$. Discrete Fourier transform of image is :

$$F(k_1, k_2) = \sum_{n_1 n_2} f(n_1, n_2) W_{N_1}^{k_1 n_1} W_{N_2}^{k_2 n_2} \quad (1)$$

$$= A_F(k_1, k_2) e^{j\theta_F(k_1, k_2)}$$

$$G(k_1, k_2) = \sum_{n_1 n_2} g(n_1, n_2) W_{N_1}^{k_1 n_1} W_{N_2}^{k_2 n_2} \quad (2)$$

$$= A_G(k_1, k_2) e^{j\theta_G(k_1, k_2)}$$

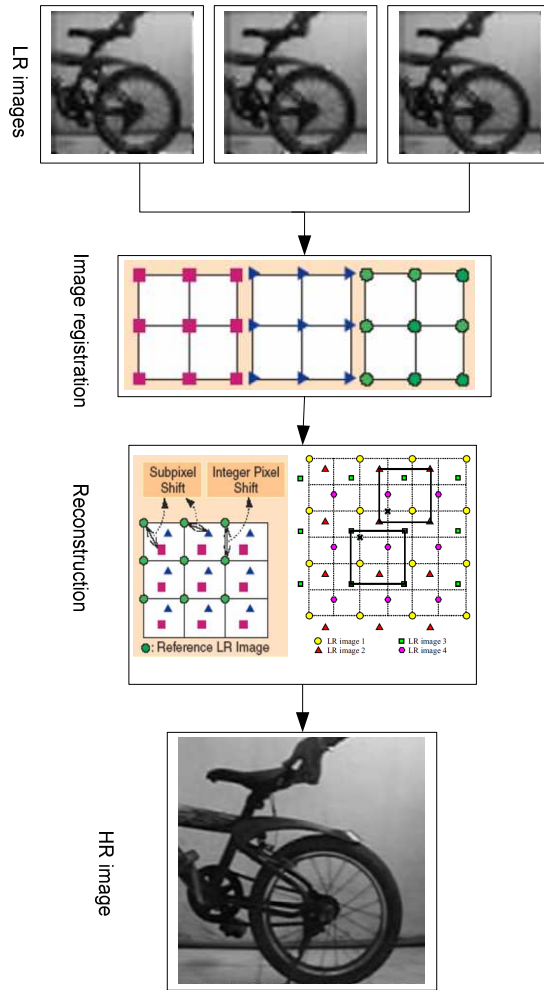


Figure 2. Stages of the superresolution

In this case :

- $F(k_1, k_2)$ and $G(k_1, k_2)$ denote Discrete Fourier Transforms (DFT) from spatial domain $f(n_1, n_2)$ and $g(n_1, n_2)$
- n_1 and n_2 are element index in spatial domain at $f(n_1, n_2)$
- k_1 and k_2 are element index in frequency domain at $F(k_1, k_2)$
- $k_1 = -M_1, \dots, M_1, k_2 = -M_2, \dots, M_2$
- $A_F(k_1, k_2)$ and $A_G(k_1, k_2)$ is the amplitude component
- $e^{j\theta_F(k_1, k_2)}$ and $e^{j\theta_G(k_1, k_2)}$ is the phase component.

- operator $\sum_{n_1 n_2}$ show $\sum_{n_1=-M_1}^{M_1} \sum_{n_2=-M_2}^{M_2}$
- $W_{N_1} = e^{j\frac{2\pi}{N_1}}$, $W_{N_2} = e^{j\frac{2\pi}{N_2}}$
- j is imaginary component

Cross spectrum phase $\hat{R}(k_1, k_2)$ defined in equation (3) as

$$\hat{R}(k_1, k_2) = \frac{F(k_1, k_2) \overline{G(k_1, k_2)}}{|F(k_1, k_2) G(k_1, k_2)|} = e^{j\theta(k_1, k_2)} \quad (3)$$

Phase-Based 2D Inverse of a function $\hat{R}(k_1, k_2)$ shown in the following equation :

$$\hat{r}(n_1, n_2) = \frac{1}{N_1 N_2} \sum_{k_1 k_2} \hat{R}(k_1, k_2) W_{N_1}^{-k_1 n_1} W_{N_2}^{-k_2 n_2} \quad (4)$$

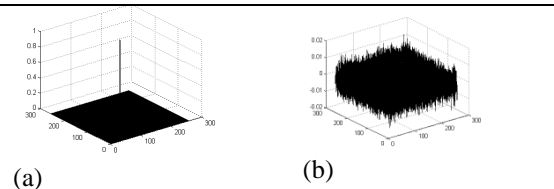


Figure 3. (a) PBIM graphs for identical image
(b) PBIM graphs for not identical image

The results of Phase-Based Functions for the function $f(n_1, n_2)$ and $g(n_1, n_2)$ which images are identical, it is obtained height of the dominant graph as shown above. While for the function which images are not identical, it is obtained graph that do not have the dominant height

Figure 3 shows a graph of two images which are identical and not identical. The identical image, has a value cross phase spectrum high, while the other one, no value cross phase spectrum high.

The coordinates of the cross spectrum of the highest phase, expressed in units of pixels translation between two images. For example, the highest peak position of a graph PBIM located at coordinates (1,2) This indicates, the first image and second image of a global translation in direction as far as 1 unit in x and 2 units in y direction.

2.2. Sub-Pixel Level Translation

Image is processed using a computer is a digital image. During the digitizing process, many of information is lost, one of which is pixels



translation. At continuous images, pixels translation are in the form of real number, but after digitizing, real translation information is lost. Therefore, we need a way to get the actual translation. One method to obtain the actual translation is by fitting of the function PBIM.

At phase correlation, sub-pixels translation will be searched by performing iteration around the peak position. Fitting the function can be used to obtain the actual translation, which is [8][9]:

$$\bar{r}(n_1, n_2) \equiv \frac{\alpha}{N_1 N_2} \frac{\sin[\pi(n_1 + \delta_1)]}{\sin\left[\frac{\pi}{N_1}(n_1 + \delta_1)\right]} \frac{\sin[\pi(n_2 + \delta_2)]}{\sin\left[\frac{\pi}{N_2}(n_2 + \delta_2)\right]} \quad (5)$$

In fitting process it is use least square quadratic, in order to obtain the value δ_1 and δ_2 which are translation in the sub pixel level. In this case :

- $N_1 \times N_2$ is dimension of images
- n is element in matrix $N_1 \times N_2$
- δ is a shift in the subpixel level
- $\alpha \leq 1$

3. HIGH RESOLUTION IMAGE RECONSTRUCTION

After a series of low-resolution image was registered to obtain the displacement of pixels, then the parameters translational and rotational displacement the images will be used for the reconstruction process. One image in a series of low-resolution image will be used as a reference in the reconstruction. Translational and rotational parameters values pixel displacement is used for projection on a grid of high resolution image. In the next section it will be reviewed the reconstruction algorithms, SANC and POCs algorithms.

3.1. Structure-Adaptive Normalized Eonvolution Algorithm (Sanc)

SANC algorithm is an image interpolation algorithms that work on the scope of Normalized convolution. The next process searches basic functions derived from the value of certainty in these images. After that the values are operated by equation (6). The operation is the Normalized convolution process.

$$p = (B^T W B)^{-1} B^T W f \quad (6)$$

To create sharper image, the process should be repeated, but with the addition of other parameters, such as estimate local image structure and scale.

Therefore, these parameters must be known in advance and then made into image density. In addition, the function is created using gaussian applicability function anisotropic. This iteration process is called the Structure Adaptive Normalized convolution.

Normalized convolution is a technique to modelling the projection of the local signals into a single set of basis functions. Although there are lots of basis functions that can be used, but the commonly used basis functions is the polynomial basis $\{1, x, y, x^2, y^2, xy, \dots\}$, where $1 = [1 \dots]^T$ (N series), $x = [x_1 x_2 \dots x_N]^T$, $y = [y_1 y_2 \dots y_N]^T$ and so forth, which reconstructed from the local coordinates of N samples of input. The use of polynomial basis functions makes Normalized convolution become the same with the expanded local Taylor series. The center of local neighbourhood is in the equation $S_0 = (x_0, 0)$, while the intensity value is in the position of $s = (x+x_0, y+y_0)$ that approximated by an extended polynomial.

$$\hat{f}(s, s_0) = p_0(s_0) + p_1(s_0)x + p_2(s_0)y + p_3(s_0)x^2 + p_4(s_0)xy + p_5(s_0)y^2 + \dots \quad (7)$$

where (x, y) is the local coordinates of the samples associated with the center s_0 . $(s_0) = [p_0 p_1 p_2 \dots p_m]$. Where s_0 is the projection coefficient of the polynomial basis function relationships at s_0 .

Adaptive Structures Normalized convolution system uses the information on the structure and distance between the actual image data input to increase the level of the Normalized convolution.

The equation (8) and (9) below are used to obtain Gradient the Structure Tensor (GST) in order to build an adaptive kernel in pixels output in the local structure of image.

$$GST = \nabla I \nabla I^T = \begin{bmatrix} I_x^2 & I_x I_y \\ I_x I_y & I_y^2 \end{bmatrix} = \lambda_u u u^T + \lambda_v v v^T \quad (8)$$

$$\phi = \arg(u), A = \frac{\lambda_u - \lambda_v}{\lambda_u + \lambda_v} \quad (9)$$

Where ϕ is main axis and A is the intensity of the anisotropic. Both of them are calculated from the eigenvector u, v that correspondd to the eigenvalue

$\lambda_u \geq \lambda_v$. $I_x = \frac{\partial I}{\partial x}$, where $I_y = \frac{\partial I}{\partial y}$ is the gradient correspondent. Other important characteristics of the data are the local sample density, because it illustrates how much

information that available at grid points near the high-resolution.

The adaptive applicability function is an anisotropic Gaussian function which the main axis is rotated to adjust the orientation of the local dominant.

$$\alpha (s, s_0) = \rho ((s - s_0)) \exp \left[- \left(\frac{x \cos \theta + y \sin \theta}{\sigma_u (s_0)} \right)^2 - \left(\frac{-x \cos \theta + y \sin \theta}{\sigma_v (s_0)} \right)^2 \right] \quad (10)$$

Where $s_0 = x_0, 0$ is the central of this analysis, $s - s_0 = x$ is the local coordinate input samples associated with s_0 , while ρ is a pillbox function that centered at the origin which restricts the kernel to certain radius. In equation (10), σ_u and σ_v are the scales of the Anisotropic Gaussian kernel. σ_u is the scale that extends along the orientation and greater than or equal to σ_v . Then both scales are adjusted to the local scale σ_c .

$$\sigma_u = \frac{\alpha}{\alpha + A} \sigma_c, \sigma_v = \frac{\alpha + A}{\alpha} \sigma_c \quad (11)$$

Parameters and functions used for high-resolution image reconstruction should use enough characteristic of image structure and detail of information, while the shape and size of the local neighborhood can be set adaptively.

3.2. Projection Onto Convex Sets Algorithm (Pocs)

Another algorithm in image reconstruction that quite effective to improve the quality of image with blur and noise is POCs.

POCs is not just a fairly simple algorithm, but it also can provide more detailed information of the reconstructed image. This algorithm is the iterative approach to perform the repetitive use of information from a series of low-resolution image and limiting the set of solutions to convex [14,15]

If a signal $f(x, y)$ and the set of convex C_i assumed to be an element in Hilbert space, then $C_i \in H, i = 1, 2, \dots, m$

and $f \in C_0 = \bigcap_{i=1}^m C_i$, provided that the slices in

C_0 not zero. Given a set of constraints on C and the

projection operator P_i in each $f(x, y)$ then obtained

$$f_{k+1} = T_{C_m} T_{C_{m-1}} \dots T_{C_1} f \quad (12)$$

Where $T_{C_i} = I + \lambda_i (P_{C_i} - I)$ the projection operator P_{C_i} projecting the signal $f(x, y)$ to the set of convex C_i dan λ_i is the multiplier with a value of $0 < \lambda_i < 2$. (equation 12).

Low-resolution image $g(x, y)$ used can be modeled as a high resolution image $f(x, y)$ who experienced a shift (s_x, s_y) and undergo a process of degradation or blurring by a point spread function $h(x, y)$ and the addition of noise $N(x, y)$ as the following equation:

$$g(x, y) = h(x, y) f(x + s_x, y + s_y) + N(x, y) \quad (13)$$

So that the set of equations is obtained convex C_i as follows:

$$C_i = \{f : |g(x, y) - h(x, y) f(x, y)| \leq N(x, y)\} \quad (14)$$

Completion of the equation (14) is obtained by iteration of orthogonal projection to a convex set defined by the constraints of low-resolution image noise level, then the projection operator which is obtained substituted into equation (11) to obtain the following equation :

$$f_{k+1} = f_k + \lambda_i \frac{g_i - h_i' f_k}{\|h_i\|^2} h_i \quad (15)$$

where g_i is i th element of vector

$g(x, y)$ and h_i' is a line to i of matrix $h(x, y)$.

An initial high resolution image called the Image Super Resolution (SRI) is projected sequentially onto the set of constraints that are built around the components of the observation image $g(x, y)$ the so called low-resolution image (LRI). Projections made in the frequency domain.

Figure 4 shows an illustration of the POCs in the frequency domain. On the right side of the circuit depicted low resolution image (LRI), which through the process to define the image preprocessing is important and will be used in the reconstruction process, if all the image used then this process can be by passed.

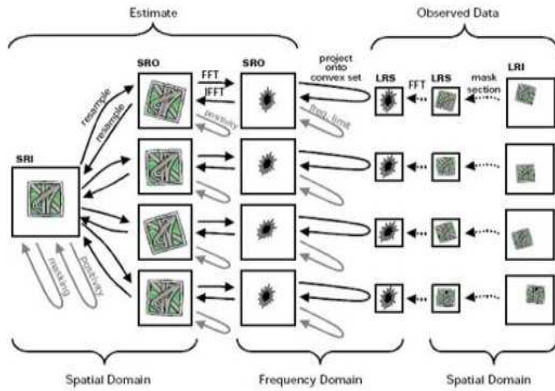


Figure 4. Illustration of POCs in the frequency domain

LRI to be used in the process of reconstruction in the Fourier transform into LRS. On the left is defined initial high-resolution image (SRI) obtained from the LRI which has been scaled or from a simple interpolation methods as nearest, bilinear, or bicubic. SRI in the re sample to adjust to the LRI, in this case when the rotation the LRI experience on SRI is also subject to rotation. SRI then transformed with a Fourier transform image Super Resolution Overlay (SRO).SRO later in the projection in order to set constraints are defined using the LRS.

4. RESULT AND DISCUSSION

The purpose of this experiment was to get the best performance of collaboration between PBIM, Keren and Marcel registration with SANC and POCs reconstruction algorithm.



Figure 5. Test images

The scenarios of testing in this study are as follows : (a) a test image in (figure 5) was assumed to be a high-resolution image; (b) image downsampling was performed to obtain image with low resolution; (c) in addition to lowering the resolution, downsampling also produced a number of image in the same scene; (d) a number of these images were registered using PBIM, Keren and Marcel, then reconstruction of the registration was used to produce a high resolution image; (e) finally, the results of this reconstruction was compared to the test images to obtain the value of PSNR.

Table 1 shows the PSNR values of image registration using PBIM collaboration and reconstruction using two reconstruction algorithms, POCs algorithm and SANC algorithm.

Table 1. PSNR results, SR with POCs Reconstruction algorithm

Num of images	POCs Reconstruction Algorithm		
	Registration		
	PBIM	Keren	Marcel
4	31.4865	31.4956	30.8905
10	32.25	31.4819	31.4956
20	32.2499	31.8698	30.9888
30	32.2495	31.8697	30.9888
50	32.2486	32.0532	30.9863
100	32.2478	32.0532	30.3825
Avg	32.12205	31.8039	30.9554

There are six experiments results from collaboration of three registration, PBIM, Keren and Marcel registration algorithm with variant LR images. Table 1 also shows the highest average of PSNR that achieved in collaboration between PBIM registration with POCs algorithm and has PSNR average value of 32.12205.

Collaboration between Keren registration and POCs algorithm reconstruction has an average PSNR value of 31.8039. The Marcel registration has an average PSNR value of 30.9554 while Keren and Marcel registration has lower PSNR value than the PBIM registration. It shows that the registration PBIM is better than Keren and Marcel registration.

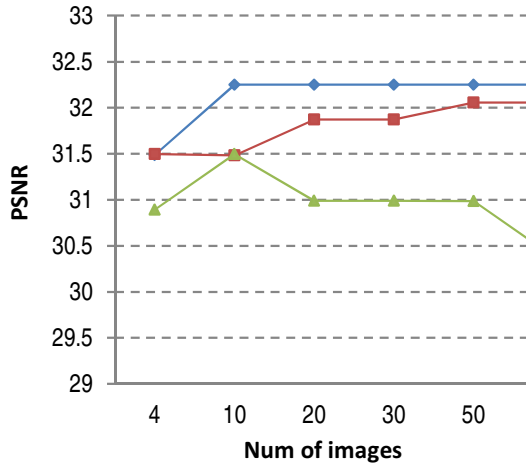
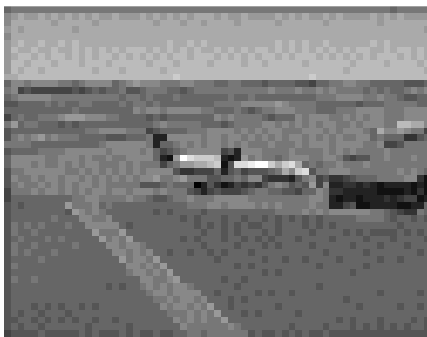


Figure 6. PSNR graph for POCs reconstruction Algorithm

Figure 6 presents a graph of the relationship between PSNR value and the number of reference images used for reconstruction. Image used in this experiment is an aircraft image (figure 7a). While Figure 7b shows the SR results using PBIM Registration with POCs reconstruction algorithm.



(a) LR images



(b) HR, output of SR

Figure 7. The result of SR

The results of this test are presented in Table 2. This table shows a comparison between PBIM, Keren and Marcel registration, which collaborated with the SANC reconstruction algorithm. The results show that PBIM registration with fitting function has a higher PSNR values compared with Keren and Marcel registration.

Table 2. PSNR results, SR with SANC Reconstruction algorithm

Num of images	SANC Reconstruction Algorithm		
	PBIM	Keren	Marcel
4	31.597	31.4553	31.0116
10	32.0968	31.4032	30.1018
20	32.0838	31.2691	29.9189
30	32.2367	31.3164	29.9964
50	32.2098	31.3197	29.9068
100	32.2154	31.3037	29.8825
Avg	32.07325	31.3445	30.1363

Figure 8 shows the relationship between PSNR value and various numbers of reference images, and collaboration between PBIM and various of registration.

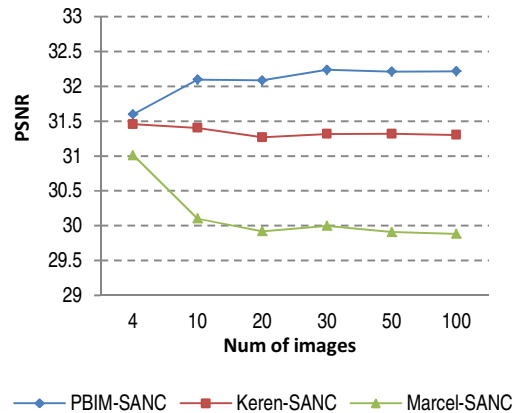


Figure 8. PSNR graph for SANC reconstruction Algorithm

Figure 9 shows the SR results for real image. Figure 9(a) is an image was extracted from video, taken with DCR-HC52E, 30 fps Sony handycame.



(a) LR image



(b) HR, output of SR

Figure 9. The result SR from real images

While Figure 9(b) show our SR result with PBIM registration.

5. CONCLUSION

Studies and experiments related to the collaboration between registration and reconstruction algorithm have been performed and obtained the following conclusions : (a) In the experiment with a number of different reference images, the collaboration between PBIM registration and POCs reconstruction algorithms has the highest PSNR average of 32.12205, while the average value of PSNR for collaboration between PBIM registration and SANC reconstruction algorithm has the highest PSNR average of 32.07325 (b) The number of images to be referenced in a high-resolution image reconstruction is not linear with the desired quality have been tested in this experiment (c) The result of PBIM registration with function fitting experiment has an average PSNR value higher than the Keren and Marcel registration

REFERENCES :

- [1] Sung Cheol Park, Min Kyu Park, and Moon Gi Kang, "Super-Resolution Image Reconstruction : A Technical Overview" *IEEE Signal Processing Magazine*, 21 Mei 2003
- [2] Z.Barbara, F Jan "Image registration methods: a survey", *Image and Vision Computing* 21, 977-1000, 2003
- [3] Barreto, D, Alvarez, Abad, "Motion Estimation Techniques in Super resolution Imager Reconstruction . A Perfomance Evaluation", *Virutal observatory : Plate Content Digitization and Image Sequence Processing*, 2005
- [4] Kenji Takita, Takashumi, Yoshisumi, "High-Accuracy Subpixel image Registration Based on Phased Only Corelation", *IECE Trans Fundamental*, Vol E86-A No 8 August 2003
- [5] Kenji Takita, Muhammad Abdul Muquit, "A Sub Pixel Correspondence Search Technique for Computer Vision Applications", *IECE Trans Fundamentals Vol.E87 No.8 Aug 2004*
- [6] F.Hassan, B.Z Jossiane "Extension of Phase Correlation to Subpixel Registration" *IEEE Transaction on Image Processing*, Vol 11, No 3, March 2002
- [7] Yi Liang,"Phased Correlation motion Estimation", *Final Project Stanford University*, 2000
- [8] GZ. Mannuel, T. Thurman Samuel, and R. Fienup James "Efficient subpixel image registration algorithms", *Optics Letters / Vol. 33, No. 2 / January 15, 2008*
- [9] Tiemao, Lin., Xuyuan, Zheng. "Super-resolution Reconstruction of MR Image Based on Structure-adaptive Normalized Convolution". *ICSP IEEE*, 2010.
- [10] Tuan, Pham. "Robust Fusion of Irregularly Sampled Data using AdaptiveNormalized Convolution". *EURASIP Journal on Applied Signal Processing*, 2006.
- [11] Chong Fan, Jianjun Zhu, Jianya Gong, Cuiling Kuang. "POCS Super-Resolution Sequence Image Reconstruction Based on Improvement Approach of Keren Registration Method". *Sixth International Conference on Intelligent Systems Design and Applications (ISDA'06) isda. vol. 2, 2006*
- [12] Hong Yu, Ma Xiang, Huang Hua, Qi Chun, "Face Image Super-resolution Through POCS and Residue Compensation", *The Institution of Engineering and Technology*, 2008



- [13]G Eran, Z Zeev, "Single-Image Digital Super-Resolution A Revised Gerchberg-Papoulis Algorithm" *IAENG International Journal of Computer Science*, 34:2, *IJCS_34_2_14*, November 2007
- [14]Deepesh Jain, "Superresolution using Papoulis-Gerchberg Algorithm", *Digital Video Processing Stanford University, Stanford, CA*, 2005
- [15]AP Sakinah, "Single Frame Image Recovery for Super Resolution with Parameter Estimation of Pearson Type VII Density" *IAENG International Journal of Computer Science*, 38:1, *IJCS_38_1_07*, February 2011
- [16]Park, Jae-Mine, Jung, Jae-Seung, dkk, "A Study on superresolution Image reconstruction for effective Spatial identification", *The Journal Of GIS Association of Korea*, Vol 13 No 4 pp.345-354, December 2005
- [17]Balaji Narayanan, C.Hardi, Kenneth E Barnner, "A Computational Efficient Super Resolution Algorithm for Video Processing Using Partition Filters", *IEEE Transactions on Circuits and Systems for Video Technology*, Vol. 17 No. 5 May 2007